

Crustal deformation rates in central and eastern U.S. inferred from GPS

Weijun Gan¹ and William H. Prescott

U.S. Geological Survey, Menlo Park, California

Abstract. Analysis of continuous GPS observations between 1996 and 2000 at 62 stations distributed throughout the central and eastern United States suggests that the area is generally stable. Seven of the 62 stations show anomalous velocities, but there is reason to suspect their monument stability. Assuming the remaining 55 stations are stable with respect to interior North America, we have found the North America-ITRF97 Euler vector ($-1.88^\circ \pm 1.04^\circ N, 77.67^\circ \pm 0.39^\circ W, 0.201^\circ \pm 0.004^\circ \text{ Myr}^{-1}$) that minimizes the RMS station velocity. Referred to fixed North America, all of these velocities are less than 3.2 mm yr^{-1} . Motion of several stations suggests the Mississippi embayment may be moving southward away from the rest of the continent at a rate of $1.7 \pm 0.9 \text{ mm yr}^{-1}$. The motion of the embayment produces a large gradient in velocity which, in turn, implies the highest seismic moment accumulation rate that we found. Although the highest rate is only marginally significant, the fact that it occurs near New Madrid, where earthquake risk is thought to be high, argues that the anomaly may be real. Nevertheless, the identification of the anomaly remains tentative.

Introduction

The central and eastern United States are within the stable interior of the North America plate, which has widely been assumed to be rigid. Very low relative velocities between geodetic stations as well as lack of apparent active surface tectonics [*e.g.* Zoback *et al.*, 1985; Argus and Gordon, 1996; Dixon *et al.*, 1996] within the area support this view. However, the occurrence of large historic earthquakes such as the 1811-1812 New Madrid earthquakes and 1886 Charleston earthquake suggests that this area is not completely stable. While there are reports of high strain rates in the New Madrid area [Liu *et al.*, 1992], the current consensus appears to be that rates are very low [Newman *et al.*, 1999; Kenner and Segall, 2000]. Here we attempt to determine whether there are regions with anomalous deformation rate within central and eastern U.S. and, if so, whether they correspond to seismically active area?

Data and Processing Techniques

Since 1994, under the coordination of the National Geodetic Survey, a nation-wide Continuously Operating Reference

¹On leave from the Institute of Geology, China Seismological Bureau, Beijing, 100029.

This paper is not subject to U.S. copyright.
Published in 2001 by the American Geophysical Union.

Paper number 2001GL013266.

Stations (CORS) network has been constructed from high quality GPS reference stations operated by a consortium of agencies. As of 2000, the CORS network included about 160 stations distributed all around the United States, most of them in the South Plains, Great Lakes, East Coast and West Coast regions of the conterminous United States [Snay and Weston, 1999].

We collected the available data from 56 CORS stations including one additional station RLAP from the Strain in Mid-America (SIMA) Continuous GPS Network, and 6 IGS tracking stations within central and eastern U.S. (Figure 1). The time series and velocities for these stations are shown on the web site at <http://quake.wr.usgs.gov/docs/deformation/EasternUS>. Although daily data for the CORS are available, we have generally only processed every seventh day's data, so as to reduce the processing time. For the IGS stations, we have processed daily solutions. All of the IGS stations have a time span of ~ 7 years, and the CORS have a time span of 4-5 years, but the station RLAP where the time span is 3 years. RLAP is located in the New Madrid seismic zone, near the epicenters of the 3 large historic earthquakes in 1811-1812.

For efficiency, we divided the 56 CORS into several subnets and processed each subnet independently. The detailed data processing technique and strategy for each subnet has been described by Prescott *et al.* [2001]. After getting the

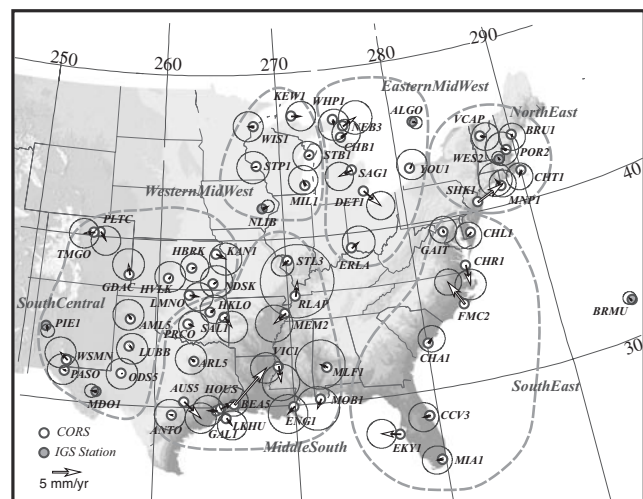


Figure 1. Map showing the locations of the CORS network in central and eastern U.S. The velocities of the individual stations relative to a North America-fixed reference frame are shown by arrows. The 95% confidence ellipse is shown at the tip of the arrow. The dashed curves roughly outline the different tectonic regimes for which we calculate uniform principal strain and rotation rates (Table 2).

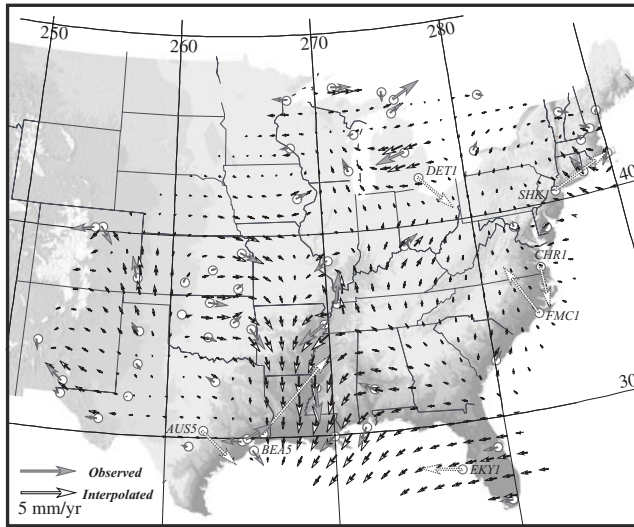


Figure 2. Map showing the velocity field of central and eastern U.S. from the interpolation algorithm spline in heavy tension. The dashed open arrows are the anomalous velocities omitted from our observed data set.

loosely constrained position solutions of the local CORS of each subnet plus ~ 44 IGS stations in ITRF97, we used the adjustment program QOCA [Dong *et al.*, 1998] (see also the web site <http://sideshow.jpl.nasa.gov:80/~dong/qoca>) in the global mode to combine them to find the optimum velocities of all the CORS and IGS tracking stations in ITRF97. In the adjustment, we partially considered the possible temporal correlations among the GPS solutions of different days. The velocities are listed in Table 1.

North America Euler Pole

In order to highlight the interior deformation of central and eastern United States, we rotated the velocities from the ITRF97 into a North America fixed reference frame. To define a North America-ITRF97 Euler pole we have found the rotation that reduced the RMS velocity for our network to a minimum. We first used all the 62 ITRF97 velocities to find an initial Euler pole ($-0.59^\circ \pm 1.60^\circ N, 78.00^\circ \pm 0.56^\circ W, 0.204^\circ \pm 0.007^\circ \text{Myr}^{-1}$). Because our velocities have an average uncertainty of $\bar{\sigma} = 1.2 \text{ mm yr}^{-1}$ (Table 1), we assumed that stations with residuals less than 3.6 mm yr^{-1} (that is, $\sim 3\bar{\sigma}$) are stable (not affected by local tectonic movement or monument instability) and eligible to be used to define the Euler pole. Excluding the 7 stations with residuals greater than 3.6 mm yr^{-1} (AUS5, BEA5, CHR1, DET1, EKY1, FMC1 and SHK1), we find the best-fitting Euler pole ($-1.88^\circ \pm 1.04^\circ N, 77.67^\circ \pm 0.39^\circ W, 0.201^\circ \pm 0.004^\circ \text{Myr}^{-1}$). This result agrees well with the recent one ($-0.9^\circ \pm 4.1^\circ N, 79.8^\circ \pm 1.6^\circ W, 0.192^\circ \pm 0.009^\circ \text{Myr}^{-1}$) derived by DeMets and Dixon [1999] using 16 permanent GPS station in ITRF96. Finally, we rotated all the 62 vectors about our Euler pole to obtain the velocities referred to stable North America (Figure 1, Table 1).

Information from the National Geodetic Survey strongly supports the suspicion that the motion of all the seven sites with anomalous residuals are due to unstable monuments rather than to tectonic motion. The sites BEA5 and AUS5 either mount their antennas on 5-meter-tall steel towers or 5-

Table 1. Site Velocities in Central and Eastern U.S. (unit: mm/yr)

| Sta. | Long. | Lat. | ITRF97 | | N.A. Fixed | |
|-------------------------|---------------|--------------|------------------|------------------|-------------|-------------|
| | | | $V_N \pm \sigma$ | $V_E \pm \sigma$ | V_N | V_E |
| ALGO ¹ | 281.93 | 45.96 | -0.5±0.5 | -15.8±0.5 | -0.3 | 0.6 |
| AML5 | 258.12 | 35.15 | -8.4±1.2 | -12.9±1.3 | 0.8 | -0.6 |
| ANTO | 261.42 | 29.49 | -7.9±1.2 | -11.4±1.3 | 0.1 | -0.5 |
| ARL5 | 262.94 | 32.76 | -7.0±1.2 | -12.7±1.3 | 0.5 | -0.7 |
| AUS5² | 262.24 | 30.31 | -10.8±1.2 | -7.9±1.3 | -3.1 | 3.3 |
| BEA5² | 265.82 | 30.16 | 0.7±1.2 | -5.1±1.2 | 7.1 | 6.3 |
| BRMU ¹ | 295.30 | 32.37 | 5.6±0.5 | -12.4±0.5 | 0.5 | -0.2 |
| BRU1 | 290.05 | 43.89 | 2.6±1.1 | -16.0±1.1 | -0.5 | -0.1 |
| CCV3 | 279.46 | 28.46 | -1.2±1.2 | -12.6±1.2 | -0.1 | -1.4 |
| CHA1 | 280.16 | 32.76 | 0.0±1.1 | -12.0±1.1 | 0.8 | 0.7 |
| CHB1 | 275.53 | 45.65 | -1.9±1.1 | -15.3±1.1 | 0.7 | 1.1 |
| CHL1 | 284.91 | 38.78 | 0.6±1.1 | -15.2±1.1 | -0.5 | -0.7 |
| CHR1² | 283.99 | 36.93 | -3.2±1.2 | -13.9±1.3 | -3.9 | 0.1 |
| CHT1 | 290.05 | 41.67 | 2.0±1.1 | -15.9±1.1 | -1.0 | -0.7 |
| DET1² | 276.91 | 42.30 | -5.4±1.1 | -12.6±1.1 | -3.2 | 2.9 |
| EKY1² | 277.24 | 27.60 | -1.3±1.2 | -14.6±1.2 | 0.6 | -3.7 |
| ENG1 | 270.06 | 29.88 | -6.1±1.6 | -12.9±1.6 | -1.3 | -1.4 |
| ERLA | 275.39 | 39.02 | -1.7±1.3 | -13.1±1.3 | 1.0 | 1.4 |
| FMC1² | 283.32 | 34.70 | 5.3±1.1 | -15.7±1.1 | 4.8 | -2.4 |
| GAIT | 282.78 | 39.13 | 0.7±1.1 | -14.7±1.1 | 0.5 | 0.0 |
| GAL1 | 265.26 | 29.33 | -8.0±1.2 | -10.1±1.2 | -1.4 | 1.0 |
| GDAC | 257.82 | 37.78 | -7.3±1.3 | -13.4±1.3 | 2.0 | -0.4 |
| HBRK | 262.71 | 38.30 | -7.4±1.1 | -13.2±1.1 | 0.1 | 0.4 |
| HKLO | 264.14 | 35.68 | -6.4±1.1 | -12.2±1.2 | 0.6 | 0.7 |
| HOUS | 264.57 | 29.78 | -6.8±1.2 | -13.0±1.2 | 0.1 | -1.8 |
| HVLK | 260.89 | 37.65 | -7.8±1.2 | -13.0±1.2 | 0.4 | 0.2 |
| KAN1 | 264.60 | 39.13 | -7.7±1.3 | -12.2±1.3 | -0.9 | 1.8 |
| KEW1 | 271.38 | 47.23 | -4.4±1.2 | -14.8±1.2 | -0.1 | 1.8 |
| LKHU | 264.85 | 29.91 | -5.4±1.2 | -8.8±1.2 | 1.4 | 2.4 |
| LMNO | 262.52 | 36.69 | -7.8±1.1 | -11.4±1.1 | -0.2 | 1.8 |
| LUBB | 258.16 | 33.54 | -9.7±1.2 | -11.4±1.3 | -0.5 | 0.4 |
| MDO1 ¹ | 255.99 | 30.68 | -9.8±0.5 | -11.8±0.5 | 0.1 | -1.1 |
| MEM2 | 269.79 | 35.47 | -6.6±1.5 | -15.6±1.5 | -1.8 | -2.4 |
| MIA3 | 279.84 | 25.73 | -0.9±1.1 | -11.5±1.2 | 0.0 | -1.2 |
| MIL1 | 272.11 | 43.00 | -2.8±1.2 | -15.9±1.2 | 1.1 | -0.4 |
| MLF1 | 272.61 | 32.09 | -3.1±2.0 | -13.6±2.0 | 0.7 | -1.4 |
| MNP1 | 288.14 | 41.07 | 3.9±1.4 | -16.0±1.4 | 1.6 | -0.9 |
| MOB1 | 271.98 | 30.23 | -5.8±1.8 | -12.5±1.8 | -1.8 | -0.9 |
| NDSK | 264.36 | 37.38 | -6.5±1.3 | -12.9±1.3 | 0.4 | 0.6 |
| NEB3 | 275.85 | 46.32 | -1.1±1.3 | -14.0±1.3 | 1.4 | 2.5 |
| NLIB ¹ | 268.43 | 41.77 | -4.9±0.5 | -13.9±0.5 | 0.5 | 1.0 |
| ODS5 | 257.69 | 31.87 | -9.4±1.2 | -11.3±1.3 | -0.1 | 0.0 |
| PASO | 253.59 | 31.77 | -10.6±1.2 | -11.4±1.3 | 0.2 | -0.5 |
| PIE1 ¹ | 251.88 | 34.30 | -12.2±0.5 | -11.2±0.6 | -1.0 | 0.2 |
| PLTC | 255.27 | 40.18 | -11.8±1.2 | -12.2±1.2 | -1.6 | 1.1 |
| POR2 | 289.29 | 43.07 | 3.2±1.3 | -16.5±1.3 | 0.4 | -0.8 |
| PRCO | 262.48 | 34.98 | -8.0±1.2 | -11.6±1.2 | -0.4 | 0.9 |
| RLAP | 270.66 | 36.47 | -1.6±2.9 | -13.1±3.0 | 2.9 | 0.5 |
| SAG1 | 276.16 | 43.63 | -3.3±1.1 | -18.5±1.1 | -0.9 | -2.7 |
| SAL1 | 265.18 | 35.37 | -8.5±1.3 | -11.6±1.3 | -1.9 | 1.3 |
| SHK1² | 285.99 | 40.47 | 3.9±1.1 | -9.5±1.1 | 2.4 | 5.5 |
| STB1 | 272.69 | 44.80 | -3.9±1.2 | -16.5±1.2 | -0.1 | -0.5 |
| STL3 | 270.24 | 38.61 | -5.6±0.9 | -15.3±0.9 | -0.9 | -1.1 |
| STP1 | 268.10 | 44.30 | -5.6±1.3 | -16.4±1.3 | -0.1 | -0.8 |
| TMGO | 254.77 | 40.13 | -10.7±1.2 | -15.3±1.2 | -0.4 | -2.0 |
| VCAP | 287.42 | 44.26 | 1.7±1.1 | -15.1±1.1 | -0.3 | 0.9 |
| VIC1 | 269.08 | 32.33 | -8.2±1.5 | -11.9±1.5 | -3.1 | 0.3 |
| WES2 ¹ | 288.51 | 42.61 | 2.8±0.5 | -15.6±0.5 | 0.5 | -0.1 |

Table 1. continued.

| Sta. | Long. | Lat. | ITRF97 | | N.A. Fixed | |
|------|--------|-------|------------------|------------------|------------|-------|
| | | | $V_N \pm \sigma$ | $V_E \pm \sigma$ | V_N | V_E |
| WHP1 | 275.04 | 46.77 | -3.8±1.3 | -16.6±1.3 | -1.0 | 0.0 |
| WIS1 | 267.99 | 46.70 | -5.4±1.2 | -17.4±1.2 | 0.1 | -1.2 |
| WSMN | 253.65 | 32.40 | -9.4±1.2 | -12.6±1.2 | 1.3 | -1.5 |
| YOU1 | 281.03 | 43.23 | 0.2±1.2 | -15.4±1.2 | 0.7 | 0.4 |

¹ IGS tracking stations.

² The stations with “abnormal” velocities (bold printed). The uncertainty of the velocities is approximately the same in both reference frames when ignoring the uncertainty of the Euler vector.

foot-tall metal stands on rooftops. The sites FMC1, SHK1, CHR1, EKY1 and DET1 use as many as three 10-foot-tall sections of commercially available Rohn 55G towers as structures on which to mount antennas. Because these towers are mainly located at the coastline, they are subjected to strong winds. We exclude the seven stations from the further discussion in this paper. Note, however, there are other equally poorly monumented stations in the network.

Velocity Field

In order to visualize the velocity field, we use the “spline in tension” technique ($\tau = 0.95$) [Wessel and Bercovici, 1998] to interpolate the velocities onto a $1^\circ \times 1^\circ$ (latitude and longitude) grid. On the velocity field map (Figure 2), the most interesting feature is that the Mississippi embayment seems to be moving southward away from the rest of the continent. Several stations are responsible for this southward motion, MEM2, located near Memphis, Tennessee, VIC1, near Vicksburg, Mississippi, MOB1, near Mobile, Alabama, and ENG1, near English Turn, Louisiana (Figure 1 and Table 1). For all these stations, the southward component is 1-2 mm yr⁻¹ with 1 sigma uncertainties of 1.3-1.5 mm yr⁻¹. Thus at best, the individual velocities are either not significant or marginally significant at the 95% confidence level. However, the southward motion of nearly all the stations near the embayment, coupled with an absence of such motion in other stations leads us to suspect that it might be real. The average southward velocity of these four stations is 1.7±0.9 mm yr⁻¹ (taking into account correlation between the stations). This rate is right at the 95% confidence level; however, we believe our error bars are conservative (i.e. too large). So the motion may be significant. Finally, the motion

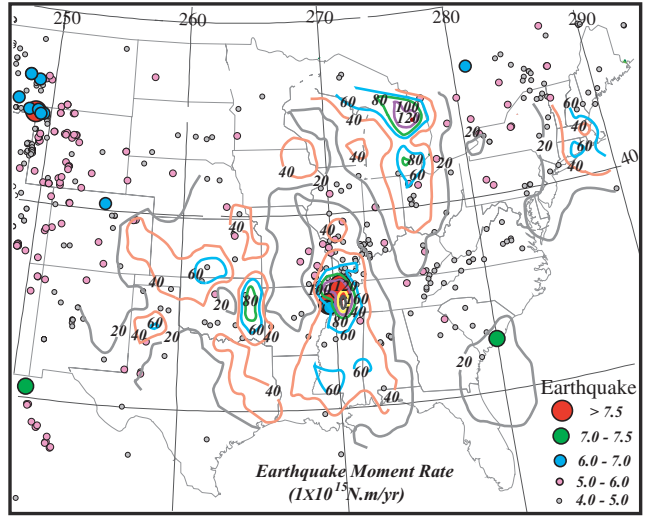


Figure 3. Map showing the seismic moment accumulation rate and historic earthquakes ($M_s \geq 4.0$) of central and eastern U.S. The contour interval is 2.0 ± 10^{16} N m yr⁻¹. The three red large dots and a blue dot in central U.S. are the epicenters of the New Madrid earthquakes (1811-1812). The green dot on the eastern south coast is the epicenter of the Charleston earthquake (1886).

of MEM2 appears to be confirmed by early results from the denser SIMA continuous GPS network, but the record from most of those SIMA stations is less than one year in length. A fifth station RLAP, just to the north of MEM2, has a quite different motion, which suggests that the anomalous southward motion of the embayment terminates at about the location of the New Madrid seismic zone. However, RLAP has a relatively large uncertainty (Figure 1 and Table 1).

Strain Rate Field

We divided central and eastern United States into six subregions based on tectonic regime (Figure 1) and calculated the average principal strain and rotation rates of the whole area and each subregion (Table 2). The results (Table 2) show that the averaged strain accumulation rates in the different tectonic regimes are all within 1-2 nanostrain yr⁻¹, except the NorthEast subregion (Figure 1) where the strain and rotation rates are as large as ~5 nanostrain (radian) yr⁻¹, but with uncertainty of the same order. None of the strain rates, including maximum shear rate ($\dot{\epsilon}_1 - \dot{\epsilon}_2$) and dilatation rate ($\dot{\epsilon}_1 + \dot{\epsilon}_2$), are significant at two standard deviations.

Table 2. Uniform Principal Strain and Rotation Rates for Subregions and Whole Region

| Region | $\dot{\epsilon}_1$ nanostrain/yr | $\dot{\epsilon}_2$ nanostrain/yr | $\dot{\omega}$ nanoradian/yr | $\dot{\epsilon}_1 - \dot{\epsilon}_2$ nanostrain/yr | $\dot{\epsilon}_1 + \dot{\epsilon}_2$ nanostrain/yr |
|----------------|-------------------------------------|-------------------------------------|---------------------------------|--|--|
| WesternMidWest | -0.0±3.1 N18°E±71° | -1.4±1.6 N72°W±71° | -1.1±1.7 | 1.4±3.5 | -1.4±3.5 |
| EasternMidWest | 1.6±1.7 N01°E±21° | -1.7±1.8 N89°W±21° | -0.3±1.2 | 3.3±2.5 | -0.1±2.5 |
| NorthEast | -1.9±4.1 N56°E±71° | -4.7±5.4 N34°W±71° | 4.6±3.4 | 2.8±6.8 | -6.6±6.8 |
| SouthEast | 0.5±0.6 N35°W±36° | -0.3±0.8 N55°E±36° | 0.1±0.5 | 0.8±1.0 | 0.2±1.0 |
| MiddleSouth | 1.5±1.6 N53°E±16° | -1.9±1.0 N37°W±16° | 0.5±0.9 | 3.4±1.9 | -0.4±1.9 |
| SouthCentral | 1.2±0.6 N19°E±14° | -0.9±0.9 N71°W±14° | 0.2±0.5 | 2.1±1.1 | 0.3±1.1 |
| All | 0.2±0.2 N44°W±13° | -0.4±0.2 N46°E±13° | 0.1±0.1 | 0.6±0.3 | -0.2±0.3 |

Extension reckoned positive. Quoted uncertainties are standard deviations.

Earthquake Hazard

To investigate in more detail nonuniform strain accumulation and the potential earthquake risk of central and eastern United States, we calculated the uniform principal strain rate in each $1^\circ \times 1^\circ$ (latitude and longitude) grid, using the interpolated velocities at the grid points [Savage *et al.* 2001, Appendix]. The strain rate was transformed to a seismic moment accumulation rate map (Figure 3) based on the formula [Savage and Simpson, 1997]

$$M_o = 2\mu AH_S \text{Max} (|\dot{\epsilon}_1|, |\dot{\epsilon}_2|, |\dot{\epsilon}_1 + \dot{\epsilon}_2|) \quad (1)$$

where M_o is the seismic moment accumulation rate; μ is the elastic layer rigidity; H_S is the seismogenic thickness; A is the area of the concerned region; $\dot{\epsilon}_1$ and $\dot{\epsilon}_2$ are the principal surficial extension and contraction rates. H_S and μ are assumed to be 11 km and 3×10^{10} N m⁻², respectively. Figure 3 shows that within a background of low seismic moment rate (between 4.0×10^{15} – 6.0×10^{16} N m yr⁻¹) there are two outstanding subregions: one is near New Madrid, with values as large as 1.0×10^{17} – 1.6×10^{17} N m yr⁻¹ and the other is in northern Michigan, with values as large as 1.0×10^{17} – 1.2×10^{17} N m yr⁻¹. To test how significant these values really are, we carried out a Monte Carlo simulation, in which we assumed the actual velocities of 55 stations were zero, and added to each velocity component an observational error drawn from a normal distribution with 0 mean and 1.5 mm yr⁻¹ standard deviation. Based on 1000 trials, we find that about 95 % of the seismic energy accumulation rates are below 8.0×10^{16} N m yr⁻¹, and about 5% are within 8.0×10^{16} – 1.2×10^{17} N m yr⁻¹. That is, a seismic moment rate below the 8.0×10^{16} N m yr⁻¹ is not significant at our measurement precision.

The high seismic moment rate around New Madrid is driven by two stations MEM2 and RLAP whose velocities are ~ 3.0 mm yr⁻¹ but oppositely directed. As discussed above, there are independent data that tends to confirm the motion of MEM2, but no independent confirmation of the motion of RLAP. A moment rate of 1.0×10^{17} – 1.6×10^{17} N m yr⁻¹ around New Madrid implies a repeat time of ~ 500 years for a $M_W 7.1$ – 7.2 event [Hanks and Boore, 1984]. Alternatively to generate a $M_W 8.0$ event would require 7,000 to 11,200 years. This of course assumes that strain rate is consistent over time and that the loading observed at the surface represents what is going on at depth.

Conclusions

Although the maximum seismic moment rate shown in Figure 3 is only marginally significant, the coincidence of that maximum with the New Madrid area, the most seismically active area in central and eastern U.S., suggests that the localization of the seismic moment accumulation in Figure 3 may be real. Based on the velocity map, it appears that the Mississippi embayment may be moving south away from the rest of the continent at a rate of 1.7 ± 0.9 mm yr⁻¹, and the northern boundary of the moving block may be in the vicinity of the New Madrid earthquakes. The area of high seismic moment accumulation in Michigan (Figure 3) has not been seismically active. The moment accumulation

there is driven by two stations NEB3 and SAG1, whose velocities are 2.8 mm yr⁻¹. Neither of the nearby stations (WHP1 and CHB1) is moving significantly. Thus the high seismic moment rate in the Michigan subregion is suspect. The region around the 1886 Charleston earthquake does not show a seismic moment accumulation rate above background value (3.0×10^{16} N m yr⁻¹).

Acknowledgments. We are grateful to the National Geodetic Survey (NGS) and other members of CORS who made the observation data available. We thank Richard Snay and Mike Cline, NGS, for providing the monument and antenna information of the stations we were concerned about. We also thank Danan Dong for his assistance in using his adjustment program QOCA.

References

- Argus, D.F., and R.G. Gordon, Tests of the rigid-plate hypothesis and bound on intraplate deformation using geodetic data from Very Long Baseline Interferometry, *J. Geophys. Res.*, *101*, 13,555-13,572, 1996.
- Dixon, T.H., A. Mao, and S. Stein, How rigid is the stable interior of the North American plate?, *Geophys. Res. Lett.*, *23*, 3035-3038, 1996.
- DeMets, C. and T.H. Dixon, New kinematic models for Pacific-North America motion from 3 Ma to present, I: Evidence for steady motion and biases in the NUVEL-1A model, *Geophys. Res. Lett.*, *26*, 1921-1924, 1999.
- Dong, D., T.A. Herring, and R.W. King, Estimating regional deformation from a combination of space and terrestrial geodetic data, *J. Geodesy*, *72*, 200-214, 1998.
- Hanks, T. C. and D. M. Boore, Moment-magnitude relations in theory and practice, *J. Geophys. Res.*, *89*, 6,229-6,238, 1984.
- Liu, Lanbo, M. D. Zoback and P. Segall, Rapid intraplate strain accumulation in the New Madrid seismic zone. *Science*, *257*, 1666-1669, 1992.
- Kenner, S. J. and P. Segall, A mechanical model for intraplate earthquakes: Application to the New Madrid seismic zone. *Science*, *289*, 2329-2332, 2000.
- Newman, A., S. Stein, J. Weber, J. Engeln, A. Mao and T. Dixon, Slow deformation and lower seismic hazard at the New Madrid seismic zone, *Science*, *284*, 619-621, 1999.
- Prescott, W.H., J.C. Savage, J.L. Svarc and D. Manaker, Deformation across the Pacific-North America plate boundary near San Francisco, California, *J. Geophys. Res.*, *106*, 6673-6682, 2001.
- Savage, J.C. and R.W. Simpson, Surface strain accumulation and the seismic moment tensor, *Bull. Seism. Soc. Am.*, *87*, 1345-1353, 1997.
- Savage, J.C., Weijun Gan, and J.L. Svarc, Strain accumulation in the Eastern California shear zone, *J. Geophys. Res.*, (in press), 2001.
- Snay R. and N. Weston, Future directions of the national CORS system, *Proceedings of the 55th Annual Meeting of the Institute of Navigation, Cambridge, MA*, June, 301-305, 1999.
- Wessel, P., and D. Bercovici, Interpolation with spline in tension: a Greens Function approach, *Mathematical Geology*, *30*, 77-93, 1998.
- Zoback, M. D., W. H. Prescott and S. W. Krueger, Evidence for lower crustal ductile strain localization in south New York. *Nature*, *317*, 705-707, 1985.

W. Gan and W. H. Prescott, U.S. Geological Survey, MS/977, 345 Middlefield Rd, Menlo Park, CA, 94025, USA. (e-mail: wjgan@usgs.gov, wprescott@usgs.gov)

(Received April 3, 2001; revised June 6, 2001; accepted June 28, 2001.)